

SUPER RESOLUTION OF 3D MRI IMAGES USING A GAUSSIAN SCALE MIXTURE MODEL CONSTRAINT

Rafiqul Islam, Andrew J. Lambert and Mark R Pickering,

School of Engineering and Information Technology,
The University of New South Wales at the Australian Defence Force Academy, Canberra, Australia

ABSTRACT

In multi-slice magnetic resonance imaging (MRI) the resolution in the slice direction is usually reduced to allow faster acquisition times and to reduce the amount of noise in each 2-D slice. In this paper, a novel image super resolution (SR) algorithm is presented that is used to improve the resolution of the 3D MRI volumes in the slice direction. The proposed SR algorithm uses a complex wavelet-based de-blurring approach with a Gaussian scale mixture model sparseness constraint. The algorithm takes several multi-slice volumes of the same anatomical region captured at different angles and combines these low-resolution images together to form a single 3D volume with much higher resolution in the slice direction. Our results show that the 3D volumes reconstructed using this approach have higher quality than volumes produced by the best previously proposed approaches.

Index Terms— Magnetic Resonance Imaging, Super Resolution, Gaussian Scale Mixture Model, Wavelet Regularization.

1. INTRODUCTION

Magnetic resonance imaging (MRI) is used to capture images of the human body or parts of the body for clinical purposes. An MRI scanner is capable of acquiring 2D cross-sectional images of the human body from any orientation. It is a non-invasive method and uses strong magnetic fields and non-ionizing radiation in the radio frequency range. In multi-slice MRI multiple 2D slices are captured to form a 3D volume of the desired body part. However, the resolution in the slice direction is usually reduced to allow faster acquisition times and to reduce the amount of noise in each 2-D slice. To deal with this problem, a number of image super resolution (SR) techniques have been used as a post-processing method to improve the quality of the low resolution images.

The basic idea underlying all SR algorithms is the combination of a number of low resolution blurred noisy images to produce a single higher resolution image. In recent

years, many super resolution algorithms have been proposed [1]. Within this wide area of study, medical image super resolution has emerged as a particularly active field. Several reconstruction methods have been developed to combine low resolution MRI images to produce one super resolution MRI image [2-6]. In this paper, we present a wavelet-based super resolution algorithm for MRI images which is based on the de-blurring algorithm developed by Zhang and Kingsbury [7]. Our results show that this algorithm provides superior performance for improving the accuracy of segmented volumes in 3D brain MRI data.

The remainder of the paper is organized as follows: In Section 2, we explain the de-blurring approach used in our SR approach. Our proposed extensions to this approach for generating a super-resolution volume are presented in Section 3. Section 4 is devoted to the experimental evaluation of the algorithms tested and finally our conclusions are presented in section 5.

2. IMAGE DE-BLURRING USING WAVELET-BASED REGULARIZATION

The main objective of image de-blurring algorithms is to find the solution of an ill-conditioned equation of the form [8]:

$$\mathbf{y} = \mathbf{H}\mathbf{x}_0 + \mathbf{b} \quad (1)$$

where \mathbf{x}_0 is a vector of pixel values from the original image, \mathbf{y} is a vector of pixel values from the observed blurry image, \mathbf{H} represents a convolution (i.e. block-circulant) matrix that approximates the blurring function and \mathbf{b} is a vector representing noise.

A solution to this minimization problem can be explained by first considering the case when the noise term \mathbf{b} is set to zero. The cost function for this case is given by:

$$J(\mathbf{x}) = \|\mathbf{y} - \mathbf{H}\mathbf{x}\|_2^2 \quad (2)$$

The solution that minimizes this cost function is given by the classic Landweber iteration as follows:

$$\mathbf{x}^{n+1} = \mathbf{x}^n + \tau \mathbf{H}'(\mathbf{y} - \mathbf{H}\mathbf{x}) \quad (3)$$

Now consider the case when no blurring occurs but noise is present in the system. A cost function that aims to minimize the ℓ_1 norm of the wavelet coefficients of \mathbf{x} can be used to solve this problem as follows:

$$J(\mathbf{x}) = \|\mathbf{y} - \mathbf{x}\|_2^2 + \lambda \|\mathbf{W}\mathbf{x}\|_1 \quad (4)$$

where the matrix \mathbf{W} represents the wavelet transform operation and λ is a regularization parameter. The optimal solution for this function is provided by soft-thresholding of the wavelet coefficients of \mathbf{x} as follows:

$$\mathbf{x} = \mathbf{M}\Phi(\mathbf{W}\mathbf{x}, \lambda/2) \quad (5)$$

where \mathbf{M} denotes the inverse wavelet transform operation and the function $\Phi(w, t)$ is the soft-thresholding function.

Daubechies et. al. proposed a solution to the problem of estimating the value of \mathbf{x}_0 when both blurring and noise are present by using the thresholded-Landweber algorithm [9]. This approach consists of first performing the Landweber iteration with step-size τ :

$$\mathbf{z}^n = \mathbf{x}^n + \tau \mathbf{H}'(\mathbf{y} - \mathbf{H}\mathbf{x}) \quad (6)$$

and then performing the wavelet domain de-noising operation:

$$\mathbf{x}^{n+1} = \mathbf{M}\Phi(\mathbf{W}\mathbf{z}^n, \tau\lambda/2) \quad (7)$$

Vonesch and Unser improved this approach by developing the fast thresholded-Landweber (FTL) de-blurring algorithm[10]. In their approach, the original thresholded-Landweber operation is performed on a wavelet sub-band basis using different step-sizes for each sub-band as follows:

For each sub-band j perform the Landweber iteration with step-size τ_j :

$$\mathbf{z}_j^n = \mathbf{W}_j(\mathbf{x}^n + \tau_j \mathbf{H}'(\mathbf{y} - \mathbf{H}\mathbf{x})) \quad (8)$$

where the matrix \mathbf{W}_j represents the wavelet transform operation for sub-band j . Then perform the wavelet domain de-noising operation on each sub-band and apply the inverse wavelet transform to find the updated version of \mathbf{x} :

$$\mathbf{x}^{n+1} = \sum_{j \in S} \mathbf{M}_j \Phi(\mathbf{z}_j^n, \tau_j \lambda/2) \quad (9)$$

3. SUPER RESOLUTION USING A GSM MODEL CONSTRAINT

In our proposed approach we extended the FTL algorithm to include multiple observed images and sub-sampling in the image acquisition model. Hence, the objective of our super resolution algorithms is to find the solution of an ill-conditioned equation of the form:

$$\mathbf{y}_i = \mathbf{D}\mathbf{H}\mathbf{F}_i \mathbf{x}_0 + \mathbf{b}_i \quad (10)$$

where \mathbf{y}_i is a vector of pixel values from the i th observed image, \mathbf{F}_i is a warping matrix used to register \mathbf{x}_0 with \mathbf{y}_i and \mathbf{D} is a sub-sampling matrix.

To accommodate this extension we modify the Landweber iteration in (8) as follows:

$$\mathbf{z}_j^n = \mathbf{W}_j \left(\mathbf{x}^n + \tau_j \sum_{i=1..k} \mathbf{F}_i^T \mathbf{H}^T \mathbf{D}^T (\mathbf{y}_i - \mathbf{D}\mathbf{H}\mathbf{F}_i \mathbf{x}) \right) \quad (11)$$

The wavelet-domain de-noising is then performed with the following function which is based on a Gaussian Scale Mixture (GSM) model, $\Theta(\mathbf{z}, t)$ proposed by Zhang and Kingsbury in [7]:

$$\Theta(\mathbf{z}_j, \varepsilon) = \frac{(\hat{\mathbf{w}}_j^2 + \varepsilon^2) \mathbf{z}_j}{(\hat{\mathbf{w}}_j^2 + \varepsilon^2) + \sigma^2} \quad (12)$$

where $\hat{\mathbf{w}}_j$ is calculated using the bi-variate shrinkage algorithm defined in [11] on the wavelet coefficients of \mathbf{x}^n and ε is a regularization parameter.

4. PERFORMANCE EVALUATION

4.1 Experimental Procedure

We conducted experiments to evaluate the performance of the proposed super-resolution algorithm for the purposes of increasing the resolution of 3D MRI images for simulated brain MRI images. The simulated input data used was a 3D MRI brain volume from the Brain Web Simulated Database [12]. We compared the performance of our proposed algorithm with a super resolution algorithm based on directional bilateral total variation regularization (DBTV) [13] as well as the Simultaneous Additive Reconstruction Technique (SART) [14] approach as these were found to be the best performing of the recently proposed SR approaches of. The wavelet transform used in our algorithm was a 3D dual tree complex wavelet transform (DTCWT) as this transform was found to be superior to the Shannon wavelet in [7].

In our experiment, we took a 3D volume with 1mm resolution in the slice-select direction and rotated it about all three axes simultaneously by 1, 2, 3 and 4 degrees. Each of these rotated volumes was then sub-sampled by a factor of 4 in the slice select direction. Blur and noise were also added to simulate the effect of the image acquisition process. Figure 1(a) shows a slice from the original volume. In the MRI acquisition process the point spread function (PSF) is defined by the slice excitation profile function. In our experiment, the slice profile functions are approximated by Gaussian functions with the full width half maximum (FWHM) distance set to the selected slice thickness.

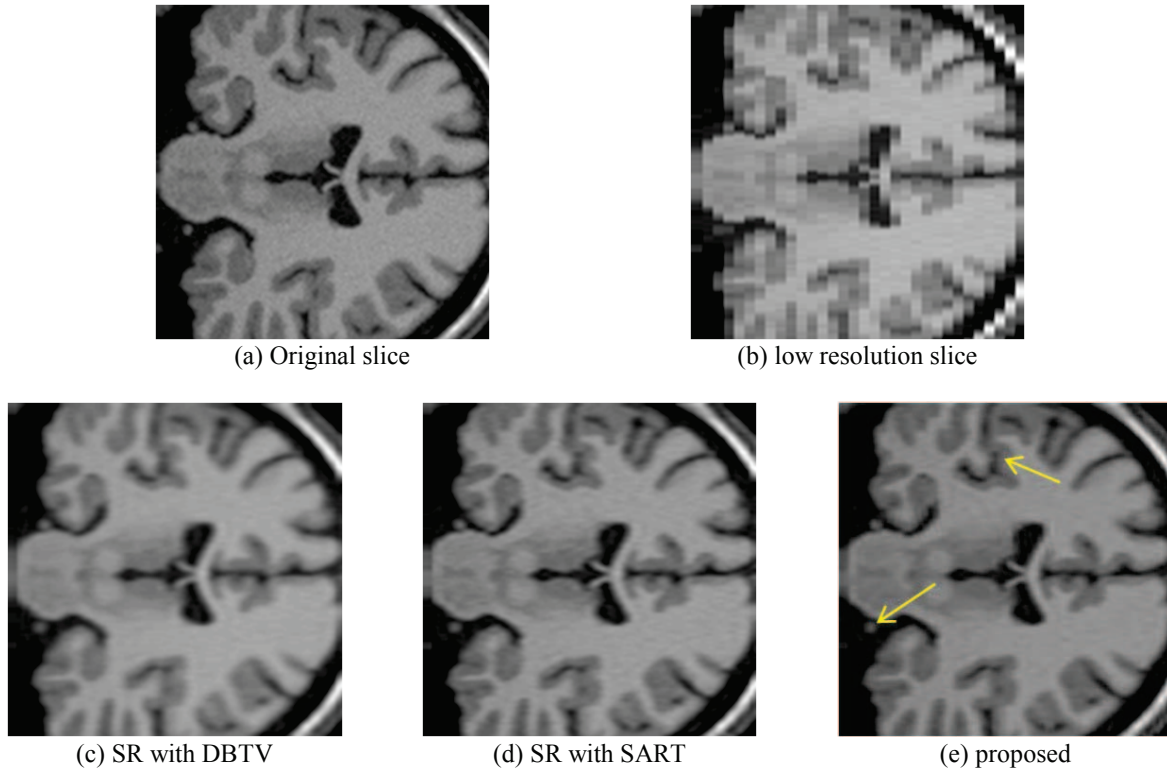


Figure 1. One slice from (a) The original volume, (b) One of the low resolution input volumes of size $128 \times 128 \times 32$ pixels, (c) The output volume for the SR with DBTV algorithm, (d) The output volume from the SR with SART algorithm and (e) The output volume for the proposed SR with GSMM constraint algorithm.

4.2 Experimental Results

Figure 1(b) shows a slice from one of the sub-sampled, blurred and noisy input volumes, Figure 1(c) shows one slice from the output of the SR with DBTV algorithm, Figure 1(d) shows one slice from the output of the SR algorithm using SART and Figure 1(e) shows one slice from the output of our proposed SR algorithm using a GSM model constraint. These images clearly show the improved subjective quality of the output of our proposed algorithm. The arrows in Figure 1(e) indicate areas of improved resolution for the proposed algorithm.

For a practical measure of the quality of the estimated super resolution volume we use a measure of the accuracy of a 3D segmented region produced using the estimated volumes. We call this measure the segmentation difference (SD) and it is defined as the percentage of voxels which are segmented differently for the estimated volume compared to the segmentation produced using the original volume. For a more standard evaluation we also compared the Peak Signal-to-Noise Ratio (PSNR) between the output volume and the original volume as a function of the iteration number.

The results of these comparisons are shown in Figure 2 and Table 1. Figure 2(a) shows a plot of the segmentation difference at each iteration when the white matter from the

estimated super-resolution volumes was segmented and compared to the segmented white matter from the original volume. Figure 2(b) shows the curves for PSNR of the estimated volume compared to the original volume for each SR technique. These results clearly show that the performance of our proposed SR algorithm using a GSM model constraint is superior to the alternative SR with DBTV and SR with SART algorithms. The PSNR values when compared with the original volume after fifteen iterations of each algorithm are shown in Table I.

TABLE I. FINAL PSNR VALUES FOR EACH ALGORITHM

Algorithms	SR with DBTV	SR using SART	SR using GSMM constraint
PSNR (dB)	40.59	41.96	42.55

5. CONCLUSIONS

In this paper, we presented a super-resolution algorithm using a Gaussian Scale Mixture Model to approximate the wavelet sparseness constraint. The algorithm takes several multi-slice volumes of the same anatomical region captured

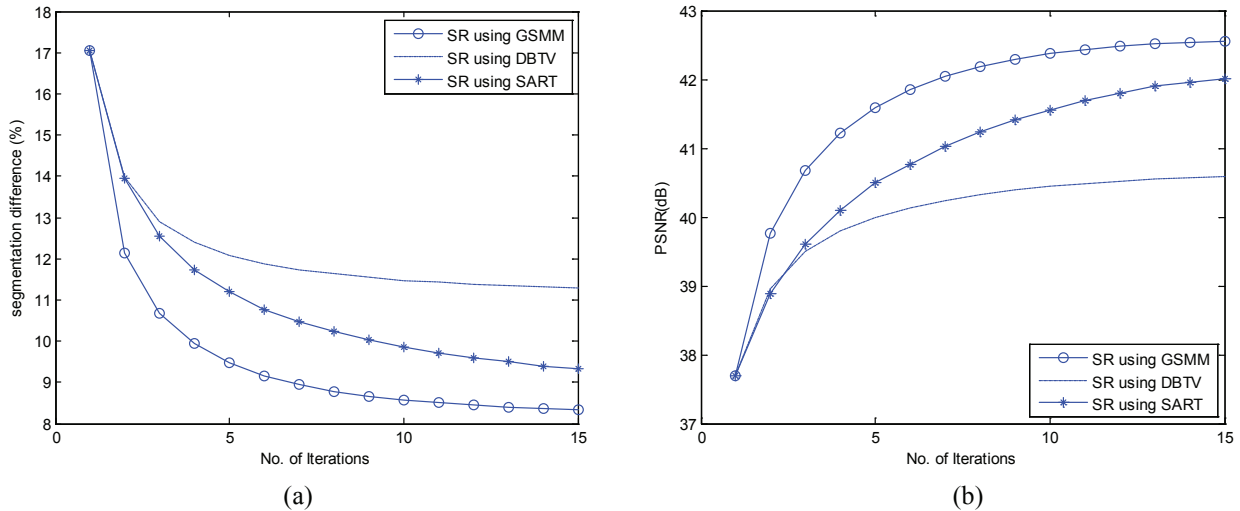


Figure 2. (a) The segmentation difference and (b) The PSNR for the SR algorithms using DBTV, SART and the proposed GSM model constraint.

at different angles and combines these low-resolution images together to form a single 3D volume with much higher resolution in the slice direction. Our results show that using this constraint provides superior performance to the alternative SR with DBTV and SR using SART approaches both visually and quantitatively.

6. REFERENCES

- [1] P. Sung Cheol, P. Min Kyu, and K. Moon Gi, "Super-resolution image reconstruction: a technical overview," *Signal Processing Magazine, IEEE*, vol. 20, pp. 21-36, 2003.
- [2] H. Greenspan, S. Peled, G. Oz, and N. Kiryati, "MRI Inter-slice Reconstruction Using Super-Resolution," in *Medical Image Computing and Computer-Assisted Intervention – MICCAI 2001*. vol. 2208, W. Niessen and M. Viergever, Eds., ed: Springer Berlin / Heidelberg, 2001, pp. 1204-1206.
- [3] S. Peled and Y. Yeshurun, "Superresolution in MRI: Application to human white matter fiber tract visualization by diffusion tensor imaging," *Magnetic Resonance in Medicine*, vol. 45, pp. 29-35, 2001.
- [4] J. T. Hsu, C. C. Yen, C. C. Li, M. Sun, B. Tian, and M. Kaygusuz, "Application of wavelet-based POCS super-resolution for cardiovascular MRI image enhancement," in *Image and Graphics, 2004. Proceedings. Third International Conference on*, 2004, pp. 572-575.
- [5] H. Greenspan, G. Oz, N. Kiryati, and S. Peled, "Super-resolution in MRI," in *Biomedical Imaging, 2002. Proceedings. 2002 IEEE International Symposium on*, 2002, pp. 943-946.
- [6] R. R. Peeters, P. Kornprobst, M. Nikolova, S. Sunaert, T. Vieville, G. Malandain, R. Deriche, O. Faugeras, M. Ng, and P. Van Hecke, "The use of super-resolution techniques to reduce slice thickness in functional MRI," *International Journal of Imaging Systems and Technology*, vol. 14, pp. 131-138, 2004.
- [7] Y. Zhang and N. Kingsbury, "Image deconvolution using a Gaussian Scale Mixtures model to approximate the wavelet sparseness constraint," presented at the Proceedings of the 2009 IEEE International Conference on Acoustics, Speech and Signal Processing, 2009.
- [8] M. Bertero and P. Boccacci, "Introduction to Inverse Problems in Imaging," ed: Taylor & Francis, 1998.
- [9] I. Daubechies, M. Defrise, and C. De Mol, "An iterative thresholding algorithm for linear inverse problems with a sparsity constraint," *Communications on Pure and Applied Mathematics*, vol. 57, pp. 1413-1457, 2004.
- [10] C. Vonesch and M. Unser, "A Fast Thresholded Landweber Algorithm for Wavelet-Regularized Multidimensional Deconvolution," *Image Processing, IEEE Transactions on*, vol. 17, pp. 539-549, 2008.
- [11] L. Sendur and I. W. Selesnick, "Bivariate shrinkage functions for wavelet-based denoising exploiting interscale dependency," *Signal Processing, IEEE Transactions on*, vol. 50, pp. 2744-2756, 2002.
- [12] D. L. Collins, A. P. Zijdenbos, V. Kollokian, J. G. Sled, N. J. Kabani, C. J. Holmes, and A. C. Evans, "Design and construction of a realistic digital brain phantom," *Medical Imaging, IEEE Transactions on*, vol. 17, pp. 463-468, 1998.
- [13] A. Ben-Ezra, H. Greenspan, and Y. Rubner, "Regularized super-resolution of brain MRI," in *Biomedical Imaging: From Nano to Macro, 2009. ISBI '09. IEEE International Symposium on*, 2009, pp. 254-257.
- [14] R. Z. Shilling, T. Q. Robbie, T. Bailloeu, K. Mewes, R. M. Mersereau, and M. E. Brummer, "A Super-Resolution Framework for 3-D High-Resolution and High-Contrast Imaging Using 2-D Multislice MRI," *Medical Imaging, IEEE Transactions on*, vol. 28, pp. 633-644, 2009.